EasyChair Preprint

№ 8575

Removal of Sulphur and Nitrogen Compounds from Model Fuel by Adsorption of Modified Activated Carbon

Narrisma Wengda Selvam

August 3, 2022

Removal Of Sulphur and Nitrogen Compounds from Model Fuel by Adsorption of Modified Activated Carbon

Narrisma a/p Wengda Selvam

No.20, Lorong Batu Nilam 13D, Bandar Bukit Tinggi 1, 41200, Klang, Selangor

narrisma99@outlook.com

Abstract. This research project is aimed to achieve highest percentage removal of DBT, QUI and IND adsorbed by double impregnated modified activated carbon. In this research project, modification of commercial activated carbon by sulphuric acid (H_2SO_4) of 15%, 30%, 45%, 60% and 75% w/v followed by subsequent 1 Zinc chloride ($ZnCl_2$): 1 activated carbon impregnation in 500°C muffle furnaces for 1 hour was carried out. Determination of best modified activated carbon is identified through highest removal of DBT, QUI and IND from adsorption experiment which were analysed using Ultra-Violet (UV-VIS). It was found that DBT and IND showed high percentage removal up to 86.23% and 82.77% respectively using 75% H_2SO_4 with $ZnCl_2$ modified AC. Meanwhile, QUI favoured 30% H_2SO_4 with $ZnCl_2$ modified AC with percentage removal of 33.17% which is still higher than unmodified AC. Physical and chemical properties such as the morphological structure, elemental analysis, porosity, pore size, surface functional group, percentage yield, pH, bulk density, content, ash content and iodine number were studied for best modified activated. Equipment such as Scanning Electron Microscope – Energy Dispersive X – Ray (SEM – EDX) and Fourier Transform Infrared Spectroscopy (FTIR) was used to characterise the modified activated carbon. A comparison between modified activated carbon and unmodified activated carbon was showed that the double impregnated modified activated carbon was successful. Langmuir, Freundlich and Temkin adsorption isotherm models as well as pseudo-first order and pseudo-second order kinetic models is considered for understanding adsorption mechanism. The research study revealed that DBT, QUI and IND followed Langmuir adsorption isotherm model with correlation coefficient, R^2 of 0.9905, 0.9791 and 0.9964 respectively. Moreover, the adsorption kinetic data of DBT, QUI and IND provided a better fitting to pseudo-second order kinetic model with R^2 of 0.9992, 0.9987 and 0.9998 respectively. According to Langmuir isotherm model and pseudo-second order kinetic model, the adsorption mechanism of DBT QUI and IND are monolayer and chemisorption process.

1. Introduction

Fossil fuels are valuable due to its efficiency in generating power particularly for transportation, power, and manufacturing industries. However, there are sulphur containing compounds (SCC) and nitrogen containing compounds (NCC) in the fossil fuels during refining process of fuel. These compounds are considered as impurities which must be removed due to its detrimental impacts to the environment and society during crude oil processing and upon combustion of gasoline and diesel oil (Chandra Srivastava, 2012). Examples of some SCC in crude oil and coal include hydrogen sulphide, benzothiophene (BT), dibenzothiophene (DBT) and 4,6-dimethyl dibenzothiophene (4,6-DMDBT) whereas examples of NCC are quinoline (QUI), indole (IND) and carbazole (CAR) (Lee et al., 2002; von Mühlen et al., 2010).

Sulphur and nitrogen compound emissions in the atmosphere are converted into acidifying chemicals such as sulphuric and nitric acid upon combustion. When these chemicals reach the ground, soil, and water, acidity arises. Soil acidity is a major contributor to danger in acidification of aquatic ecosystem and forest destruction which may endanger the lives of plant and animal species. Besides that, nitrogen oxides (NO_x) also contribute to ground-level ozone depletion and eutrophication while sulphur oxides (SO_x) cause adverse health effects to human beings such as lung cancer and eye irritation. The combination of SO_2 and NO_2 is also one of the smog and acid rain pollutants.

In the present day, catalytic hydrodesulfurization (HDS) and hydrodenitrogenation (HDN) are the typical approaches used in petroleum refining process to the reduce the sulphur and nitrogen contents in fuel. The challenges in terms of efficiency arises for the conventional HDS technology due to its ability of removing only aliphatic sulphur compounds instead of heterocyclic aromatic sulfur compound such as DBT and its derivatives which makes up more than three fourth of the total sulphur content in fuel oil (Chandra Srivastava, 2012).

Not only that, prior to ultra-deep desulfurization using HDS technology, NCCs should be eliminated from the fuels because they interfere catalytic reaction by competing with SCCs for active sites thus, lowering the activity of the catalysts (Almarri et al., 2009). In comparison with the HDS approach, HDN technology is relatively slow in terms of rate of chemical reaction. In addition, HDN technique requires the availability of hydrogen gas at relatively high temperature and pressure which increases the production cost at a large scale. Traditional methods for pollutant removal, such as HDS and HDN, are regarded uneconomical due to its high cost and numerous constraints and downsides.

Advancement of technologies have led to alternative techniques to remove SCCs and NCCs from model fuel such as oxidation, extraction, and bio-desulfurization. Another type of approach that has been garnering attention for its many advantages is the adsorption method. Adsorption is one of the most promising approaches for ultra-deep desulfurization and denitrogenation to produce cleaner fuel. Along with its low energy consumption, ability to execute at ambient temperature and pressure without the need for high pressure hydrogen gas, ability to regenerate the spent adsorbent, and is widely available, adsorptive desulfurization and denitrogenation is extensively recognised as an efficient and cost-effective way to remove organosulfur and organonitrogen compounds from model fuel (Almarri et al., 2009; Wang and Yang, 2007)

Commercial activated carbon (CAC) is historically used for adsorption of pollutants in liquid and gas phase. It has relatively larger pores which enables good adsorption capacity of impurities, is cheap and suitable for selective removal of SCC due existence of hydrogen bond (Bansal and Goyal, 2005). A study conducted by Almarri et al. (2009)concluded that activated carbon (AC) had achieved better adsorption capacity for nitrogen compound in model diesel fuel as compared to alumina-based adsorbents. Many published studies have found a way to enhance the adsorption ability of AC through physical or chemical activation.

On the other hand, modifying AC through chemical treatment using impregnation method can enhance surface adsorption capacity, therefore improving the efficiency of the activated carbon to retain atoms of impurities. Adsorption capacities of DBT in model fuel doubled using prepared activated carbon modified with Ag nanoparticles as compared to unmodified activated carbon (Olajire et al., 2017). According to Ahmed et al. (2013), MIL-100 (Cr) modified with acid treatment has led to an improvement in adsorption capacity of adsorbent to remove BT and QUI which are base adsorbates as well as IND which is a neutral adsorbate. Modified commercial activated carbon oxidized with sulphuric acid at large range of concentration has been proven to increase removal of NCCs from model fuel (Anisuzzaman et al., 2018).

Since DBT, QUI and IND are organic compounds, they have electron cloud and non-bound electron pair in their atoms which exhibit high nucleophilicity. As a result, adsorbents with acidic electrophilic properties have a higher adsorption capacity (Lopes et al., 2016). In addition to that, acid pre-treated followed by metal impregnation can improve distribution of functional groups on surface of adsorbents(Tsai et al., 2017). These past studies have led my research towards creating an AC with two step modification which is by sulphuric acid followed by zinc chloride to remove DBT, QUI and IND from model fuel. Most published studies had only study removal percentage of AC modified by

only one method of surface modification. Till date, there are insufficient studies on the effect of adsorption capacity in model fuel using modified CAC through double surface modification especially via sulphuric acid treatment followed by zinc chloride impregnation for removal of DBT, QUI, IND in model fuel. Furthermore, this study concentrates on adsorption isotherms and kinetics to comprehend the adsorptive capabilities and mechanism of this modified commercial activated carbon and compare it to other findings.

2. Methodology

This chapter explains the chemicals, apparatus, and procedures that is carried out in this proposed research study. This section is divided into six major stages, namely (i) modification of commercial activated carbon through 15%, 30%, 45%, 60% and 75% w/v H_2SO_4 followed by subsequent 1 $ZnCl_2$: 1 activated carbon impregnation; (ii) characterization of best modified activated carbon such as porosity, pore size and functional groups using SEM/EDX and FTIR; (iii) preparation of standard calibration curve for absorbance value against DBT, QUI and IND concentration between 20-100 mg/l using UV-Vis spectrophotometry; (iv) development of most suitable isotherm model (Langmuir, Freundlich and Temkin) and kinetic model (pseudo-first order and pseudo-second order) through adsorption experiment.

2.1. Preparation of Chemicals and Materials

For this experiment, DARCO® charcoal activated carbon was purchased from Sigma-Aldrich. The charcoal activated carbon (CAC) is in granular form with mesh particle size ranging from 20 to 40. The CAC has a total surface area of 650 m^2/g, ash content of ≤0.40% as well as a moisture content of ≤12%. The sulfur-based adsorbates which is dibenzothiophene (DBT) and nitrogen-based adsorbates which are quinoline (QUI) (purity, 99%) and indole (IND) (purity, 99%) were available in laboratory. The model fuel used is n-hexane (C_4H_{14}) with purity of 99% were available in laboratory as well. For surface modification of activated carbon, sulphuric acid (H_2SO_4) of (95 – 98)% purity and zinc (II) chloride ($ZnCl_2$) are readily available in chemical store.

2.2. Preparation of Commercial Modified Activated Carbon

2.2.1. Purification Step of Charcoal Activated Carbon. The AC was immersed in hot distilled water for 2 hours and then washed several times with cold distilled water to remove impurities as an additional purification step while the other chemicals was used as it is. After that, the CAC is then dried in a 120°C oven for 24 hours for complete drying and cooled in desiccator afterwards (Tsai et al., 2017).

2.2.2. Sulphuric acid (H_2SO_4) Chemical Treatment Followed by Metal Impregnation using Zinc (II) Chloride ($ZnCl_2$). There are two modification step of CAC which is by various concentration of H_2SO_4 followed by subsequent $ZnCl_2$ impregnation. The chemical treatment method is adopted from (Anisuzzaman et al., 2018) and (Tsai et al., 2017)with minor modifications. Firstly, 10 g of the CAC is pre-treated with 30 ml H_2SO_4 of 15%, 30%, 45%, 60% and 75% w/v in 100 ml beakers respectively. Then, the beakers is sealed with aluminium foil with punched holes to allow vapour evaporation. To allow for thorough dissolution, the beakers is then kept in the sonicator bath for three days. The H_2SO_4-treated CAC is filtered with filter paper and washed with distilled water before it is dried in a 120℃ oven for 24 hours to remove excess moisture.

The subsequent $ZnCl_2$ impregnation is referred from (Angin, 2014; Yakub et al., 2013). $ZnCl_2$ solution is prepared by solubilizing 10.0 g of $ZnCl_2$ solids in 250 ml distilled water. 15% H_2SO_4-treated CAC is transferred into the beaker containing $ZnCl_2$ solution for (1 $ZnCl_2$:1 H_2SO_4-treated CAC) impregnation. The flask is left to shake at 80℃ for 24 hours for complete reaction. After this, the samples are filtered using a filter paper and is left to dry at an 120℃ oven for 24 hours to remove excess zinc and chlorine. The impregnation with $ZnCl_2$ is repeated for 30%, 45%, 60% and 75% w/v H_2SO_4. The samples are then weighed using an analytical balance to record the final mass of activated carbon obtained before it is placed in an atmosphere integrated furnace.

Next, the impregnated solid was placed in an atmosphere integrated furnace at 500℃ for 1 hour for carbonization. After cooling down, the activated carbon was rinsed with 1M KOH solution to remove possible clogs of zinc and chloride from pores of activated carbon and neutralize pH of AC. Distilled water was used to rinse the modified activated carbon until the pH reaches neutral at 6-7. Finally, the prepared modified activated carbon is dried in a 120℃ oven for 24 hours before storing in glass bottle for characterization tests.

2.3. Preparation of DBT, QUI and IND Stock Solution

Stock solution for dibenzothiophene, quinoline and indole of 1000 mg/l each is prepared by dissolving 1000 mg of the adsorbates in 1 L n-hexane solution. A standard calibration curve of DBT, QUI and IND are plotted where y-axis and x-axis represents absorbance value and adsorbate concentration respectively. DBT, QUI and IND are then diluted to 20 mg/l, 40 mg/l, 60 mg/l, 80 mg/l, and 100 mg/l using dilution equation as follows:

$$\boldsymbol{M_1V_1 = M_2V_2}$$

Where, M_1 = Initial Molarity (mg/l); V_1 = Initial volume (L); M_2 = Final Molarity (mg/l); V_2 = Final volume (L)

2.4. Adsorption Experiment for Determination of Best Modified CAC

The method used for this experiment is followed from (Anisuzzaman et al., 2018; Anisuzzaman & Maramin, 2021) with slight modifications. First and foremost, 100 ml n-hexane fuel solution of DBT, QUI and IND are prepared by placing them in three separate beakers with initial concentration of 100 mg/l each. Next, 1g of Zn-impregnated CAC that was pre-treated with 15% H_2SO_4 solution is added into each beaker. Then, beakers are magnetically stirred at 160 rpm for 1 hour in an isothermal water bath at 25°C. After 1 hour of stirring, solid residues are separated with filter paper and filtered solution is analysed using UV-VIS spectrophotometry at maximum wavelength of DBT, QUI and IND.

The experiment is repeated using Zn-impregnated CAC with 30%, 45%, 60% and 75% pre-treated H_2SO_4 and unmodified CAC. The final unknown concentration of DBT, QUI and IND in n-hexane with initial concentration of 100 mg/l each were determined from the standard calibration curve of each of the adsorbates. Then, the percentage removal of DBT, QUI and IND from n-hexane by modified and unmodified CAC is calculated according to the equation stated below.

$$\boldsymbol{RP = \frac{(C_o - C_t)}{C_o} \times 100\%}$$

Where, R= Removal percentage of adsorbate from n-hexane (%); C_o = Initial adsorbate concentration (mg/l); C_t = Adsorbate concentration at a given time (mg/l)

2.5. Characterization of Best Modified Charcoal Activated Carbon

2.5.1. Percentage yield Determination. The percentage yield is calculated by taking weight of 30% and 75% H_2SO_4 and $ZnCl_2$ impregnated AC which is then divided by initial weight of activated carbon before modification which is expressed in the equation represented below (Anisuzzaman et al., 2015),

$$Percentage\ Yield = \frac{Final\ weight\ of\ modified\ activated\ carbon\ (g)}{Initial\ weight\ of\ activated\ carbon\ (g)} \times 100\%$$

2.5.2. pH Determination. The pH of modified CAC is tested using method followed by (Anisuzzaman et al., 2015), with a minor modification. First, 1.0 g of 30% and 75% H_2SO_4 and $ZnCl_2$ impregnated AC is weighed and placed in a beaker and 100 ml distilled water is added. Then, the beaker is heated to a temperature of 40°C and left to cool down to room temperature once the thermometer temperature hits 40°C. To dilute the mixture, another 100 ml distilled water is added, and the beaker is stirred. The pH value was determined by using a Mettler Toledo pH meter.

2.5.3. Bulk Density Determination. Bulk density of modified activated carbon method is determined from (Efeovbokhan et al., 2019a). Firstly, 25 ml measuring cylinder is placed on analytical balance and press 'TARE'. The modified activated carbon is then poured into the measuring cylinder until it reaches the 25 ml marking. To prevent voids, the measuring cylinder were tapped. The weight shown on the analytical balance is recorded and bulk density was calculated according to equation below.

$$Bulk\ density = \frac{Mass\ of\ modified\ activated\ carbon\ (g)}{Volume\ of\ measuring\ cylinder\ (ml)}$$

2.5.4. Moisture Content Determination. The moisture content in modified activated carbon was determined from procedure done by (Jeyakumar & Chandrasekaran, 2014). In a 110℃ oven, 1.0 g of modified activated carbon is dried for 3 hours and cooled in desiccator before weighing. The process of heating, cooling, and weighing was repeated until a constant mass of modified activated carbon is achieved. The calculation for moisture content is shown below.

$$Moisture\ content = \frac{(Initial\ mass - Final\ mass)\ g}{Initial\ mass\ (g)} \times 100\%$$

2.5.5. Ash Content Determination. The determination of ash content was done by weighing modified activated carbon right after moisture content test in a muffle furnace of 500℃ for 4 hours. Then, the ash was cooled in desiccator before re-weighing. Ash content is calculated as below (Jeyakumar & Chandrasekaran, 2014).

$$Ash\ Content = \frac{Mass\ of\ ash\ (g)}{Mass\ of\ modified\ CAC\ (g) \times \frac{(100 - \%\ Moisture\ Content)}{100}} \times 100\%$$

2.5.6. Iodine Number Determination. The iodine number was determined according to standard ASTM D460794 method. Firstly, 1.0 g of modified activated carbon was mixed with 10 ml of 5% HCL solution and boiled for 30 seconds before allowing to cool. Then, 100 ml of 0.1N iodine solution was poured into the conical flask and stirred vigorously for 30 seconds before filtering with filter paper. 50 ml of the filtrate is titrated against 0.1N sodium thiosulphate solution until solution turns pale yellow. Once pale yellow is formed, 2 ml of starch solution was added into the conical flask. When solution turned colourless, titration is stopped, and the amount of sodium thiosulphate utilized is recorded. Two important calculation is required which is represented as below. X/M presents the amount of iodine adsorbed for 1.0 g of modified activated carbon while C is the concentration of iodine in the filtered solution.

$$\frac{X}{M} = \frac{A - (DF \times B \times S)}{M}$$

Where, A = 12693 (Used sodium thiosulphate (ml) × 0.1)/100 ml; DF = (100+10) ml/50 ml = 2.2; B = 0.1N(126.93); S = Used sodium thiosulphate (ml); M = modified activated carbon dosage

$$C = \frac{0.1 \times S}{F}$$

Where, S = Used sodium thiosulphate (ml); F = Filtrate used (50 ml)

Then a graph of X/M against C was plotted for another two different dosages (2g and 3g). At C = 0.02 N on the plot, the iodine number is determined from X/M.

2.5.7. Functional Group Determination Using Fourier Transform Infrared Spectroscopy (FTIR). The functional groups and covalent bonding present in the 30% and 75% H_2SO_4 + $ZnCl_2$ modified AC as well as unmodified CAC were analyzed and compared using a Fourier Transform Infrared Spectroscopy (FTIR) model Inveio-R Bruker. This effective analytical instrument is able to identify the functional groups which could have enhanced the adsorption capability of modified CAC to remove DBT, QUI and IND from n-hexane. First, 0.5 g of 30% and 75% H_2SO_4 and $ZnCl_2$ modified AC was mounted and measured under the spectrometer. The wavenumber range were set between 400 to 4000 cm^{-1}.

2.5.8. Scanning Electron Microscope with Energy Dispersive X-Ray Analysis (SEM/EDX). The surface morphology and topography such as pore shape, pore distribution and pore size of the modified and unmodified CAC were visualized using Scanning Electron Microscope with Energy Dispersive X-Ray (SEM/EDX) model Hitachi. The direct microstructure changes on the surface of the modified CAC were able to be observed using SEM and comparisons are made with the unmodified CAC. The magnifications were adjusted from 100x to 3000x to obtain a high-resolution image. On the other hand, the EDX results is used to determine the type and amount of each element present and on both types of CAC. But before that, the 30% and 75% H_2SO_4 and $ZnCl_2$ modified AC is coated with gold using the Quorum Q150T ES plus Sputter Coater since the samples were non-conductive and beam sensitive.

2.5.9. Surface Morphology Analysis. A Java-based image processing program called ImageJ were used to analyze the surface morphology such as pore size and porosity of the 30% and 75% H_2SO_4 + $ZnCl_2$ modified AC and unmodified CAC. This software was developed by researchers from National Institutes of Health and the Laboratory for Optical and Computational Instrumentation from University of Wisconsin and can be downloaded in Microsoft Window for free. ImageJ program is relatively simple as it is designed to calculate distance, area and develop statistical graphs according to

the results. Hence, this software was utilized to identify the pore size and porosity of the captured modified and unmodified CAC images from SEM.

2.6. Adsorption Isotherm and Kinetic Models

2.6.1. Determination of Adsorption Isotherm. This research carried out batch isotherm experiments with a little modification from (Anisuzzaman et al., 2018; Anisuzzaman & Maramin, 2021) to develop most suitable isotherm model either Langmuir, Freundlich or Temkin so that the adsorption relationship between the unbounded and bounded DBT, QUI and IND on modified CAC surface can be understood further. For that, n-hexane fuel solution with varying concentration DBT, QUI and IND but constant modified CAC dosage were tested.

Firstly, 100 ml of model fuel solution consisting of 20 mg/l of DBT, QUI and IND were prepared in three separate beakers. Next, 1 g of best modified CAC were added into all beakers and magnetically stir beaker in 25°C water bath at 160 rpm for 1 hour. To separate solid residues, a filter paper is used, and the filtered solution is then analysed using UV-VIS spectrophotometry at maximum wavelength of DBT, QUI and IND. The experiment is repeated with varying concentration which is 40 mg/l, 60 mg/l, 80 mg/l and 100 mg/l of DBT, QUI and IND in 100ml n-hexane fuel solution.

The final unknown concentration of DBT, QUI and IND in n-hexane that had initial concentration of 100 mg/l each was determined from the standard calibration curve of each of the adsorbates. Then, the amount of DBT, QUI and IND at equilibrium were determined by using the equation below.

$$Q_e = \frac{(C_o - C_e)V}{W}$$

Where, Q_e = Amount of adsorbate adsorption at equilibrium (mg/g); C_o = Initial adsorbate concentration (mg/l); C_e = Equilibrium adsorbate concentration (mg/l); V = Volume of solution (L); W = Weight of modified CAC used (g)

After determining the amount of DBT, QUI and IND absorbed at equilibrium, the data was fitted to form linear graphs according to the theoretical equations of Langmuir isotherm, Freundlich isotherm and Temkin isotherm represented as below.

Langmuir model equation:

$$\frac{C_e}{Q_e} = \frac{C_e}{Q_{max}} + \frac{1}{K_L Q_{max}};\ R_L = \frac{1}{K_L C_O}$$

Where, Q_{max} = Maximum monolayer adsorption capacity (mg/g); K_L = Langmuir isotherm constant (mg/l); C_e = Equilibrium adsorbate concentration (mg/l); Q_e = Amount of adsorbate adsorption at equilibrium (mg/g); R_L = Separation factor; C_o = Initial adsorbate concentration (mg/l)

Freundlich model equation:

$$\log Q_e = \frac{1}{n}\log C_e + \log K_F$$

Where, C_e = Equilibrium adsorbate concentration (mg/l); Q_e = Amount of adsorbate adsorption at equilibrium (mg/g); n = Adsorption intensity (mg/g); K_F = Freundlich isotherm constant (mg/g)

Temkin model equation:

$$Q_e = \left[\frac{RT}{b_T}\right]\ln C_e + \frac{RT}{b_T}\ln A_T$$

Where, C_e = Equilibrium adsorbate concentration (mg/l); b_T = Temkin constant corresponding to enthalpy of sorption (kJ/mol); A_T = Temkin binding constant at equilibrium (l/mg); R = Universal gas constant (kJ/mol.K); T = Temperature (K); Q_e = Amount of adsorbate adsorption at equilibrium (mg/g)

2.6.2. Determination of Adsorption Kinetic Model. bath at 160rpm for 1 hour. To separate solid residues, a filter paper is used, and the filtered solution is analyzed using UV-VIS spectrophotometry at maximum wavelength of DBT, QUI and IND. The experiment is repeated with the following mixing time of 2 to 5 hours.

The final unknown concentration of DBT, QUI and IND in n-hexane with initial concentration of 100 mg/l each was determined from the standard calibration curve of each of the adsorbates. Then, the amount of DBT, QUI and IND at equilibrium was determined by using adsorption at equilibrium equation at given time as below.

$$Q_t = \frac{(C_i - C_t)V}{W}$$

Where, Q_t = Amount of adsorbate adsorption at equilibrium at given time (mg/g); C_i = Initial adsorbate concentration at given time (mg/l); C_t = Equilibrium adsorbate concentration at given time (mg/l); V = Volume of solution (L); W = Weight of modified CAC used (g)

After that, the data was fitted to form linear graphs according to the theoretical equations of pseudo-first order model and pseudo-second order model as below.

Pseudo-first order model equation:

$$\ln(Q_e - Q_t) = -K_1 t + \ln Q_e$$

Where, Q_t = Amount of adsorbate adsorption at time (mg/g); K_1 = Pseudo-first order adsorption rate constant (hr^{-1}); t = Mixing time (hr); Q_e = Amount of adsorb ate adsorption at equilibrium (mg/g)

Pseudo-second order model equation:

$$\frac{t}{Q_t} = \frac{t}{Q_e} + \frac{1}{K_2 Q_e^2}$$

Where, Q_t = Amount of adsorbate adsorption at time (mg/g); K_2 = Pseudo-second order adsorption rate constant (g/mg.hr); t = Mixing time (hr); Q_e = Amount of adsorbate adsorption at equilibrium (mg/g)

3. Results and Discussion

3.1. Best Modified AC

Table 1: DBT, QUI and IND Adsorption Experimental Results using Various H_2SO_4 and $ZnCl_2$ Modification

Modified AC	Percentage Removal of modified AC on adsorbates (%)		
	DBT	QUI	IND
Unmodified	82.95	20.03	64.68
15% H_2SO_4 + $ZnCl_2$	83.20	9.250	28.95
30% H_2SO_4 + $ZnCl_2$	84.12	33.17	46.16
45% H_2SO_4 + $ZnCl_2$	85.83	23.12	68.09
60% H_2SO_4 + $ZnCl_2$	86.14	20.77	74.05
75% H_2SO_4 + $ZnCl_2$	86.23	4.380	82.77

According to the table, the best modified AC for adsorbing DBT and IND is 75% H_2SO_4 pre-treated AC followed by $ZnCl_2$ modification while the best modified AC for adsorbing QUI is 30% H_2SO_4 pre-treated AC followed by $ZnCl_2$ modification. Among all adsorbates, DBT showed substantially high percentage removal using the modified AC. This could be due presence of high surface acidity on modified AC which favoured DBT removal over the other NCC adsorbates. Similar observations were reported by Lopes et al. (2016), which concluded that higher SCC (up to 75%) than NCC were removed especially by using modification with H_2SO_4. This is due to the fact that DBT is a sulphur base adsorbate that is attracted to more acid groups present on 75% H_2SO_4 + $ZnCl_2$ modified AC, thus it facilitates easier binding to large pores, hence better adsorption performance (Seredych et al., 2009). On the other hand, QUI favoured 30% H_2SO_4 concentration rather than 75% H_2SO_4 concentration

because high temperature in muffle furnace (500°C) during activation possibly removed more carboxylic acid groups that were essential for adsorption of QUI in 75% H_2SO_4 + $ZnCl_2$ modified AC where similar results was reported by Qu et al. (2016).

3.2. Physiochemical Characteristics of Modified AC

Table 2: Physiochemical characterization comparison between modified AC

Physiochemical Study	**30% H_2SO_4 $ZnCl_2$ modified AC**	**75% H_2SO_4 $ZnCl_2$ modified AC**
Percentage Yield (%)	72.08	71.13
pH	5.53	5.36
Bulk Density (g/cm^3)	0.42	0.43
Moisture Content (%)	4.88	4.46
Ash Content (%)	3.17	2.68
Iodine number (mg/g)	857	861

3.2.1. Percentage Yield. The percentage yield of best modified AC which is 30% and 75% H_2SO_4 pre-treated AC followed by $ZnCl_2$ impregnation ratio 1:1 is 72.08% and 71.13% respectively. Based on the study carried out by Anisuzzaman et al. (2018), the typical percentage yield obtained from modification with H_2SO_4 ranged between 82.88% to 97.08% where best modified AC dosage was 40% H_2SO_4. From that study, it was found that the higher H_2SO_4 dosage yielded lower AC as compared to the lower H_2SO_4 dosage. According to this experimental study, the 75% H_2SO_4 dosage modified AC resulted to a slightly lower percentage yield than the 30% H_2SO_4 dosage which is proven by Anisuzzaman et al. (2018). From the results, it can be said that the samples clearly suffered a considerable mass loss. This is most likely caused by AC oxidation, which degrades not only the inorganic constituents but as well as the organic constituents present in the AC before surface modification (Anisuzzaman et al., 2018).

According to Pratumpong & Toommee (2016), $ZnCl_2$ with impregnation ratio of 1:1 yielded the highest waste-derived AC which is at 47.82%. Another study concluded that an increase in $ZnCl_2$ impregnation ratio could increase percentage yield of waste-derived AC up to 47.08% (Awe et al., 2020). However, the observed yield from this experiment is comparatively higher than those reported in the mentioned studies. This could be due to the usage of commercial AC while the ones mentioned in the studies are waste-derived AC that contains high volatile matter that are easily burned off upon carbonization especially when oxygen and hydrogen atoms found in the carbonaceous structure, binds together, hence, forming water molecule (Bouchemal et al., 2009). This statement is proven by a study

by Yahya et al. (2015) who concluded that percentage yields of AC prepared by coal as raw material are higher than of waste-derived AC.

Chemical agents such as $ZnCl_2$ has been studied by other researchers to boost product yield and reduce burn-off. This is because $ZnCl_2$ functions as a catalyst to accelerate dehydration which is essential for promoting cross-link bonds, thus forming a rigid matrix (Iwanow et al., 2020). Due to the hard and solid structure, the modified AC is able to release lower volatile compound during carbonization, hence achieving higher AC yields. From the results, it can be said that the surface modification using H_2SO_4 and $ZnCl_2$ can prevent the production of tar and other substances which could possibly clog the pores of the AC during activation process since these activating agents has the potential to conserve carbon, minimize the loss of volatile matter and has opened pores due to the reduction in mass (Bouchemal et al., 2009).

3.2.2. pH. One of the most important parameters that has a significant impact of the adsorption of specific compounds by is the pH of the absorbent. This is because the pH of absorbent will determine the type of surface groups on AC matrix, whether it is acidic or basic (Jeyakumar & Chandrasekaran, 2014). The surface chemistry of the AC can be altered during preparation by adding chemical activating agents (Iwanow et al., 2020). Moreover, the uptake of DBT, QUI and IND are strongly dependent of the acid sites available of the surface of the modified AC (Ahmed, Hasan, et al., 2013). Since H_2SO_4 and $ZnCl_2$ are acidic compounds, the typical pH range of modified AC should be between 4 to 6 (Anisuzzaman et al., 2018; Shafiq et al., 2017). In this study, the pH for 30% H_2SO_4 pre-treated and $ZnCl_2$ modified AC were found to be 5.53 while the pH for 75% H_2SO_4 pre-treated and $ZnCl_2$ modified AC is 5.36, hence proving that the modified AC is slightly acidic.

According to (Lopes et al., 2016), the modification of AC using H_2SO_4 absorbed the high percentage of sulphur and nitrogen from commercial diesel as compared with nitric acid and hydrochloric acid due to its presence of highest number of oxygen-containing functional groups on the surface of AC which are also known as acidic groups. Another study conducted by (Ahmed, Khan, et al., 2013), confirmed that acidic conditions favoured adsorption of DBT, QUI and IND. The reason to it is because DBT and QUI are hard and soft base adsorbates respectively while IND is a neutral adsorbate. He reported that acid-modified AC improved adsorptive performance of DBT and QUI due to its strong acid-base interactions. Similarly, it was also reported by (Sarker et al., 2018), that adsorption performance of QUI and IND increased linearly with an increase in oxygenated functional groups on the absorbent.

3.2.3 Bulk Density. The bulk density of a prepared AC is an important parameter in determining its suitability for specific applications. An activated carbon with low bulk density shows that less AC is required to be filled into a given space while higher bulk densities require higher AC volume to fit into the given space. Therefore, higher bulk density carbon would result in a better adsorption performance of adsorbate as compared to low density carbon. The bulk density of raw AC was determined to be 0.38 g/cm^3 whereas, with double impregnation of 30% H_2SO_4 and $ZnCl_2$, the bulk density increased slightly to 0.42 g/cm^3. The bulk density further increased to 0.43 g/cm^3 with 75% H_2SO_4 and $ZnCl_2$ treatment.

Based on research by Efeovbokhan et al. (2019), the bulk density of AC is dependent on the activation chemical and carbonization temperature where, lower activation temperature with bio-acid activators increased bulk density of AC, indicating that adsorption capabilities were better than of bio-base activators with high carbonization temperature. This is in agreement with Yusufu M. I. (2012), which concluded that acid activation treatment can significantly increase the bulk densities of AC up to 18% for wood precursor AC. Moreover, in Gunorubon Dagde & Kekpugile (2018) study, the increment of $ZnCl_2$ concentration as an activating agent had reported a higher bulk density due to the expansion of molecules which resulted from the cross-linking reaction.

3.2.4. Moisture Content. Moisture content can be defined as the amount of water that is physically retained in the AC sample under standard conditions. The amount of moisture present in the AC of the 30% and 75% H_2SO_4 pre-treated AC followed by $ZnCl_2$ impregnation are 4.88% and 4.46% respectively. The 75% H_2SO_4 pre-treated AC followed by $ZnCl_2$ has a lower moisture content because of the higher concentration of H_2SO_4 used which promotes better dehydrating effect (Gunorubon Dagde & Kekpugile, 2018). Similar results were obtained by Owabor & Iyaomolere (2013), which also reported that increasing concentration of activating agent had decreased the moisture content in the AC due to higher dehydration rate but only until a certain limit until concentration had no influence on the moisture content. Moreover, higher acid concentration is advantageous for enhancing the surface area of AC, and thus decreasing the AC's hygroscopic characteristics (Suhdi & Wang, 2021).

According to Efeovbokhan et al. (2019), lower moisture content would contribute to higher percentage yield which is achieved in this experimental study since 30% H_2SO_4 pre-treated AC and $ZnCl_2$ has a higher percentage yield but lower moisture content. The adsorption performance of adsorbate onto modified AC is affected by the moisture content because higher moisture content would mean that more water molecules are filled in the micropores of AC therefore, inhibiting and competing with adsorbate molecules to be filled into the active sites during adsorption process. Zhou

et al. (2001) observed that higher moisture content showed a negative trend on the adsorption performance, thus lowering the efficiency of AC.

3.2.5. Ash Content. Ash content is one of the physiochemical characteristics that determines the quality of the modified AC. Ash content is the inorganic and unstable fraction of AC that does not chemically react with any components such as calcium, magnesium and silica that remains after carbonization (Jeyakumar & Chandrasekaran, 2014). The ash content of AC varies from one to another depending on the mineral compounds that is available in the precursor raw material (Iwanow et al., 2020). Generally, the ash content of an AC after chemical activation ranges from 1% to 20% depending on the type of starting material (Zulkania et al., 2018).

The presence of high ash content percentage is undesirable during AC preparation because it influences the adsorption performance due to the reduction in carbon mechanical strength (Zulkania et al., 2018). In addition to that, the purity of the carbon is reflected in the ash level which also impacts the adsorption performance by creating inactive sites and clogged pores (Martínez-Mendoza et al., 2020; Yusufu M. I., 2012). The ash content of the 30% and 75% H_2SO_4 pre-treated AC followed by $ZnCl_2$ impregnation are 3.17% and 2.68% respectively. These values are significantly higher that ash content present in commercial AC which is ≤0.40%. This indicates that ash content increased with the double impregnation using H_2SO_4 and $ZnCl_2$. This result could be attributed to the presence of remaining activating agent residuals and insoluble organic compounds entrapped in the ash along with AC (Yusufu M. I., 2012).

However, the 75% H_2SO_4 pre-treated AC with $ZnCl_2$ modification has a lower ash content due to the reaction of acid with mineral components in the AC as well as low char burn-off, hence contributing to lower ash content (Owabor & Iyaomolere, 2013; Yusufu M. I., 2012). The results of ash content in this experimental study are significantly lower than compared to previous research studies of Owabor & Iyaomolere (2013) and Gunorubon Dagde & Kekpugile (2018) in which impregnation ratio of 1:1 $ZnCl_2$ reported 4.72% and 7.80% ash content respectively. Another study by Mkungunugwa et al. (2021), observed that activation using higher H_2SO_4 concentration reduced the ash content of AC from 3.49% to 0.97% using 40% and 60% H_2SO_4 concentration respectively.

3.2.6 Iodine Number. Iodine number also known as iodine index is another crucial characterization analysis which is defined as the mass of iodine that is adsorbed by a certain weight of modified AC (on a dry basis) at an equilibrium concentration. It also provides information of degree of porosity of the modified AC. According to Jeyakumar & Chandrasekaran (2014), a higher iodine number represents a higher activation stage. Since the results are plotted on logarithmic axes, where the

corresponding iodine number can be found when residual filtrate normality is 0.02 according to the ASTM-D4607, hence it is only a rough estimate of the micropore surface area of modified AC.

The determination of iodine number is successful since the correlation coefficient values, R^2 for both graphs are above 0.995 as required in the standard. The estimated iodine number for 30% and 75% H_2SO_4 $ZnCl_2$ modified AC are 857 mg/g and 861 mg/g respectively. The iodine number of both modified AC are within the typical range of 500-1200 mg/g (Mopoung et al., 2015). The iodine number results were expected to higher for 75% H_2SO_4 $ZnCl_2$ modified AC since, a higher H_2SO_4 concentration were used for the surface modification process. Besides that, the results indicate that the 75% H_2SO_4 $ZnCl_2$ modified AC has more accessible micropore volume and large surface area as compared to the 30% H_2SO_4 $ZnCl_2$ modified AC due to slightly higher iodine number. Similarly, Yusufu M. I. (2012) reported that the iodine number increased with respect to concentration of acid utilised for surface modification of AC. In addition to that, a high iodine number of both modified AC promotes increase in pore development and thus the adsorption performance of DBT, QUI and IND from n-hexane which were conducted earlier.

3.3. FTIR Analysis. AC is typically made up of carbon atoms, but it also contains different heteroatoms such as hydrogen, oxygen, nitrogen, and sulphur (Iwanow et al., 2020). The surface functional groups and other chemical component structure contained in AC were identified using FTIR analysis, which is significant in characterising and predicting adsorption performance (Mkungunugwa et al., 2021). The spectra are recorded between the range of 4000 cm^{-1} and 400 cm^{-1}. The samples' spectra revealed the existence of various active functional groups which demonstrates a decrease, emergence, disappearance, or widening of the peaks following the impregnation procedure with 30% and 75% H_2SO_4 pre-treated AC followed by $ZnCl_2$ impregnation.

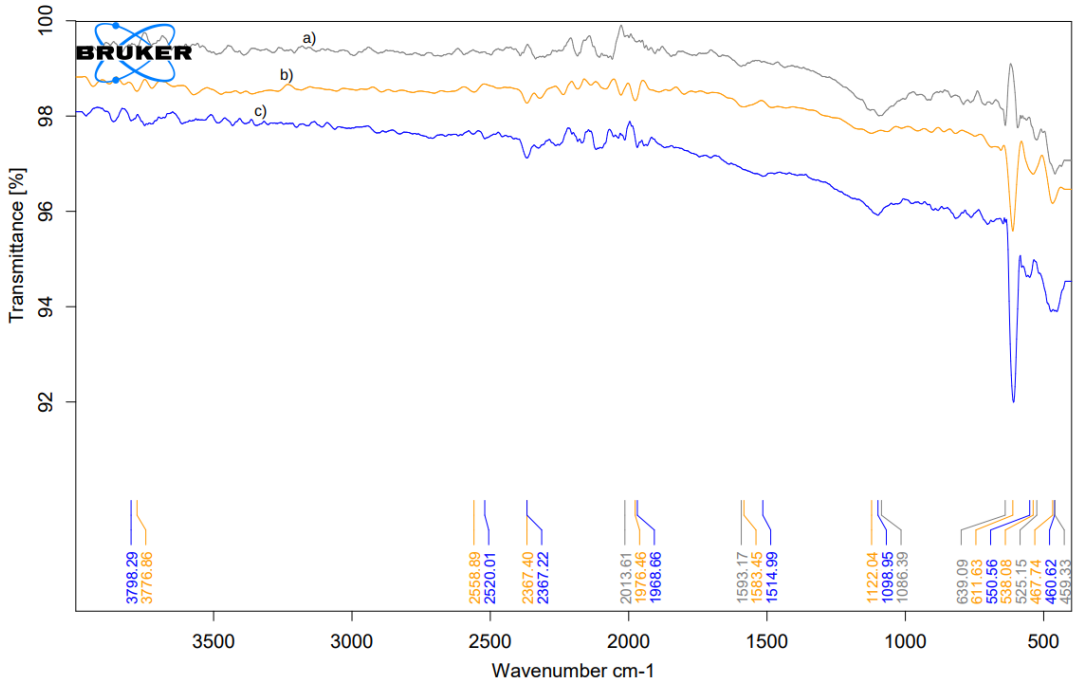

Figure 1: FTIR spectra for a) unmodified AC, b) 75% H_2SO_4 pre-treated AC + $ZnCl_2$ impregnationp, c) 30% H_2SO_4 pre-treated AC + $ZnCl_2$ impregnation

The FTIR spectra of 30% and 75% H_2SO_4 pre-treated AC followed by $ZnCl_2$ impregnation showed considerably more functional groups present of the surface of modified AC as compared to unmodified AC. It can be observed that the rise of two bandwidths between 690 cm^{-1} to 600 cm^{-1} and 1130 cm^{-1} to 1090 cm^{-1} in all FTIR spectra corresponds to S=O and S-O stretching with indication that there is presence of sulphate ion even before H_2SO_4 and $ZnCl_2$ modification . However, the peaks around 690 cm^{-1} to 600 cm^{-1} are stronger for 30% and 75% H_2SO_4 pre-treated AC and $ZnCl_2$ as compared to unmodified AC because of the high H_2SO_4 concentration used upon modification. Another common peak if for C=C weak stretching found in aromatic rings which is around 1600 cm^{-1} to 1510 cm^{-1}. The reason to it is because of the tars formed from aromatization and decomposition of C-H bonds, followed by condensation and dehydration hence, influencing formation of aromatic compounds with cross linking to generate more stable aromatic bond (Anisuzzaman et al., 2015; Mopoung et al., 2015).

The bandwidths between 2400 cm^{-1} and 1900 cm^{-1} were noted to be substantially stronger at 30% and 75% H_2SO_4 pre-treated AC and $ZnCl_2$ as compared to unmodified AC due to asymmetric or symmetric stretching in aliphatic band in -CH, $-CH_2$ or $-CH_3$. The increase in aliphatic structure is possibly caused by the extraction of OH and H functional groups from aromatic rings during the double impregnation as well as the dehydrating effect of $ZnCl_2$ (Angin, 2014). Besides that, the

presence of aliphatic group indicates that they are organic compounds which contain carbon-hydrogen bond that is able to bind to other elements including but not limited to sulphur, nitrogen, oxygen and chlorine adsorbates (Mkungunugwa et al., 2021).

The difference between unmodified AC and modified AC is the presence of S-H weak stretching representing thiol compound, found between bandwidth range of 2600 cm^{-1} to 2500 cm^{-1} only for 30% and 75% H_2SO_4 pre-treated AC and $ZnCl_2$ modified AC (Lesaoana et al., 2019). Therefore, this proves that the sulphur was successfully incorporated to form thiol compound of surface of modified AC. In addition to that, the peak observed between bandwidth of 3800 cm^{-1} to 3500 cm^{-1} represents O-H stretching, indicating presence of intermolecular bonded hydroxyl functional groups such as carboxylic acid which could be the result of H_2SO_4 surface modification, thus generating more acidic functional groups on AC surface while reducing hydroxide functional groups (Anisuzzaman et al., 2015b; Jawad et al., 2016).

3.4. Adsorption Isotherm Analysis. Three adsorption isotherm models which are Langmuir, Freundlich and Temkin is used to investigate the interaction between surface of modified AC and DBT, QUI and IND compounds when adsorption attains equilibrium at various initial adsorbate concentrations.

Table 3: Adsorption experiment data for DBT concentration

C_o (mg/l)	C_e (mg/l)	V (l)	W (g)	Q_e (mg/g)	Removal Percentage (%)
20.00	1.060	0.1000	1.000	1.894	94.70
40.00	5.366	0.1000	1.000	3.463	86.56
60.00	8.549	0.1000	1.000	5.145	85.75
80.00	17.10	0.1000	1.000	6.290	78.62
100.00	33.54	0.1000	1.000	6.646	66.46

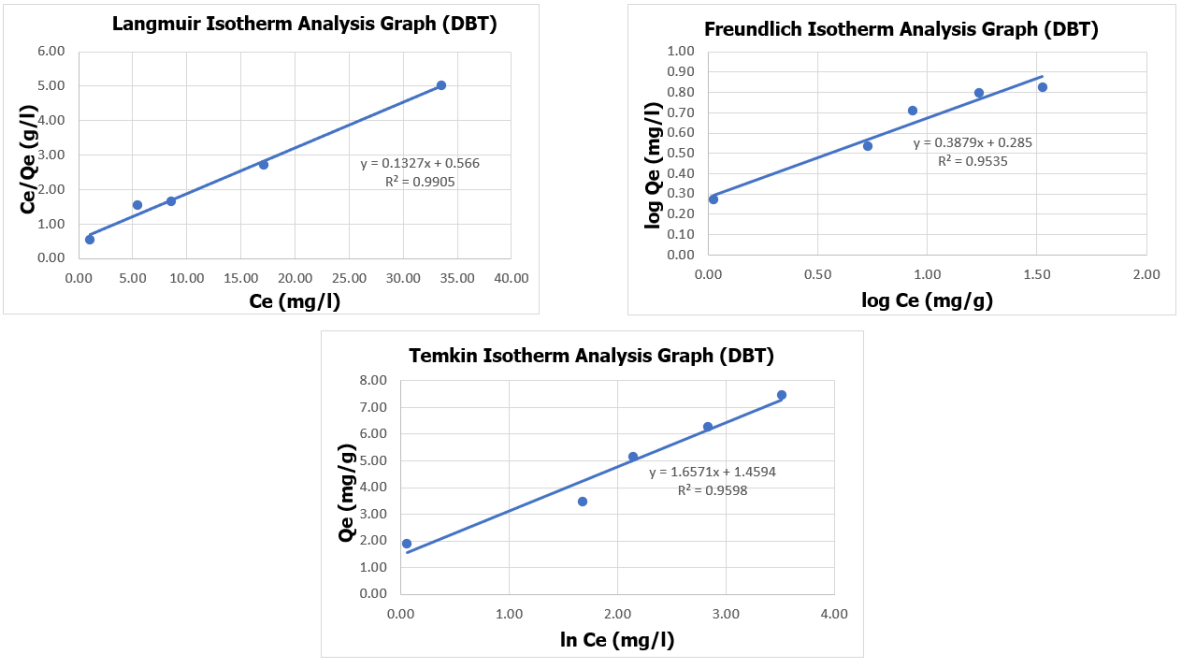

Figure 2: Isotherm analysis for DBT adsorption onto 75% H_2SO_4 with $ZnCl_2$ modified AC

According to all the isotherm graph, it can be concluded that the adsorption of DBT using 75% H_2SO_4 pre-treated AC followed by $ZnCl_2$ modification is successful. Based on the graphs, it is observed that as concentration of DBT at equilibrium increases, the adsorption capacity of DBT increases as well. This means that as initial DBT concentration increases, adsorption performance reduces where the percentage removal range of DBT from n-hexane were in between 66.46% to 94.70%. This could be because n-hexane has hydrophobic characteristic, which is heavily absorbed by the modified AC, thus influencing the efficiency of DBT removal (Olajire et al., 2017). In addition to that, the reduction in adsorptive site's density to total DBT compounds could reason to why the adsorption performance is decreasing as initial concentration increases (Anisuzzaman & Maramin, 2021).

Table 4: Langmuir. Freundlich and Temkin isotherm constants for adsorption of DBT from n-hexane

Langmuir's Constants	
K_L (l/mg)	0.2345
Q_{max} (mg/g)	7.536
R_L	0.0427-0.2133
R^2	0.9905
Freundlich's Constants	

K_F (l/mg)	1.928
n	2.578
R^2	0.9535
Temkin's Constants	
A_T (l/mg)	2.413
b_T (kJ/mol)	1.496
R^2	0.9598

The best sequence of the DBT adsorption isotherm model for this study is Langmuir > Temkin > Freundlich. As shown in Table 4, the correlation coefficient values, R^2 reveals that DBT adsorption in this experimental study fits the Langmuir isotherm equation as compared to the rest since it has is highest R^2, thereby, closer to 1 (R^2>0.99). This implies the occurrence of monolayer adsorption on limited number of homogenous active sites of 75% H_2SO_4 pre-treated and $ZnCl_2$ modified AC. K_L at 0.2007 l/mg is associated with the variation of the modified AC's appropriate area and porosity, indicating that a greater surface area and pore diameter results in a significant adsorption capacity (Ayawei et al., 2017). The separation factor, R_L indicates that the adsorption of DBT compound onto modified AC is favourable and optimum since it is ranges between 0 to 1.

Similarly, adsorption of DBT from acid activated carbon showed that Langmuir isotherm model was best suited for 20 to 100 mg/l initial concentration. On the other hand, the Freundlich isotherm model had R^2 closer to 1 in adsorption experiment of DBT using clay adsorbent with initial concentration ranging from 100 to 600 mg/l (Olajire et al., 2017). The value of n > 1 from Freundlich isotherm provides information that the adsorption mechanism is a reversible process, implying physisorption (Desta, 2013). The energy constant relating to enthalpy of sorption, b_T is relatively low at only 1.496 kJ/mol. Ha et al. (2019) reported a b_T value between 2715 to 4858 kJ/mol during adsorption experiment of DBT from gasoline and diesel using clay. The very low b_T value obtained in this experimental study may be attributed to the fact that DBT adsorption process using modified AC involves hydrophobic interaction, which does not radiate energy as readily as ionic and polar interactions, owning to dehydration/hydration behaviour (Olajire et al., 2017).

Table 5: Adsorption experiment data for QUI concentration

C_o (mg/l)	**C_e (mg/l)**	**V (l)**	**W (g)**	**Q_e (mg/g)**	**Removal Percentage (%)**
20.00	5.805	0.1000	1.000	1.419	70.97

40.00	9.545	0.1000	1.000	3.045	76.14
60.00	24.52	0.1000	1.000	3.548	59.13
80.00	39.57	0.1000	1.000	4.043	50.54
100.00	59.69	0.1000	1.000	4.031	40.31

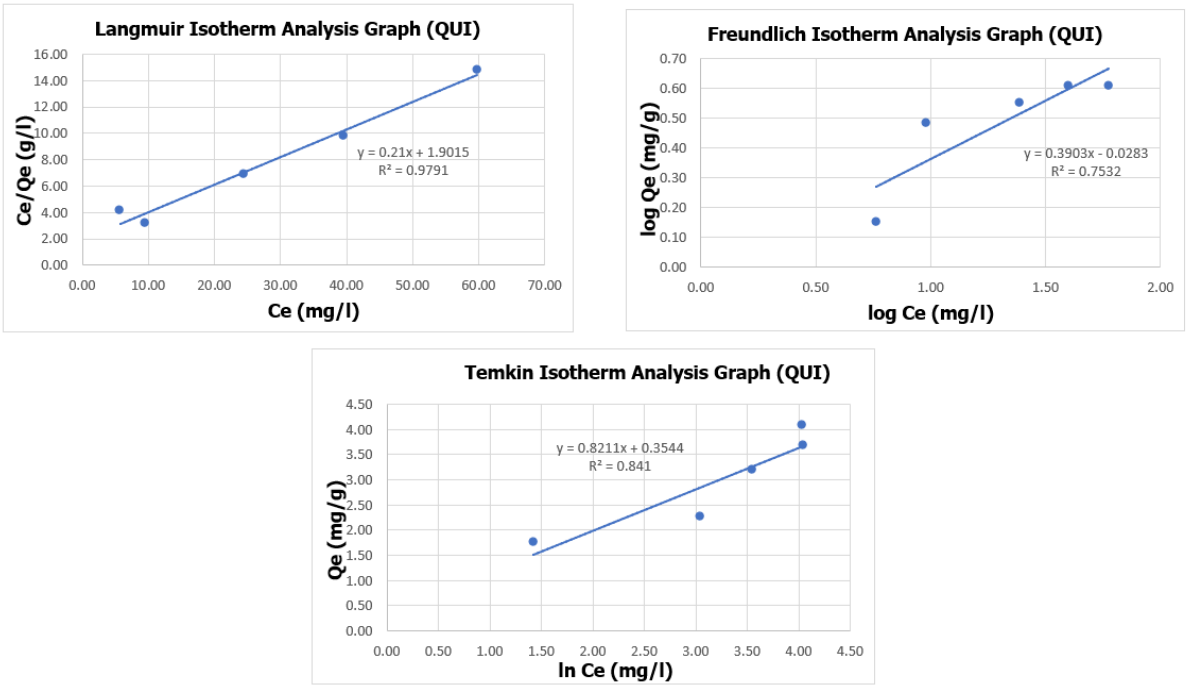

Figure 3: Isotherm analysis for QUI adsorption onto 30% H_2SO_4 with $ZnCl_2$ modified AC

The graphs shown above shows positive increase in adsorption capacity with concentration of QUI at equilibrium. This signifies that 30% H_2SO_4 and $ZnCl_2$ modified AC is capable of reducing the concentration of QUI in n-hexane. However, it was found that as initial concentration of QUI increased, the percentage removal of QUI notably decreased ranging to be between 40.31% to 76.14% where initial concentration of QUI were 40.00 mg/l and 100 mg/l respectively. In this study, it can be concluded that 30% H_2SO_4 and $ZnCl_2$ modified AC is able to effectively remove low QUI concentration in n-hexane which is between 20.00 mg/l to 40.00 mg/l. Similarly, like the adsorption of DBT onto modified AC, the reduced percentage removal could be because n-hexane has hydrophobic characteristic, which is heavily absorbed by the modified AC, thus influencing the efficiency of QUI removal (Olajire et al., 2017). Moreover, the low percentage of QUI removal at higher initial concentration is due to insufficient binding sites of QUI molecule on surface of modified AC since most active sites is already saturated with the QUI molecule.

Table 6: Langmuir. Freundlich and Temkin isotherm constants for adsorption of QUI from n-hexane

Langmuir's Constants	
K_L (l/mg)	0.1104
Q_{max} (mg/g)	4.762
R_L	0.091-0.4257
R^2	0.9791
Freundlich's Constants	
K_F (l/mg)	0.9369
n	2.562
R^2	0.7532
Temkin's Constants	
A_T (l/mg)	1.540
b_T (kJ/mol)	3.019
R^2	0.8410

The best sequence of the QUI adsorption isotherm model for this study is Langmuir > Temkin > Freundlich. The Langmuir adsorption isotherm model provided the best fitting to the adsorption data, since it has the highest R^2 value at 0.9791 compared to Freundlich and Temkin isotherm models. This reveals that QUI adsorption compromises entirely of a monolayer at surface of 30% H_2SO_4 and $ZnCl_2$ modified AC where only one QUI molecule can occupy a single active site. The Langmuir isotherm constant, K_L resulted to be 0.1104 l/mg which provides information on the interaction strength between QUI compound and modified AC surface. This experimental value is significantly higher that the K_L value reported by Anisuzzaman et al. (2018) where the modification of 40% H_2SO_4 modified AC provided a K_L value of 0.0540 mg/l. The separation factor, R_L shows that the adsorption of QUI compound onto modified AC is favourable and optimum since it is ranges between 0 to 1.

These results are consistent with other research studies which reported that the adsorption of QUI on HCL and H_2SO_4 modified AC fitted Langmuir adsorption isotherm model (Anisuzzaman et al., 2018; Anisuzzaman & Kamarulzaman, 2021). Conversely, the correlation coefficient for Freundlich isotherm model was observed to be between 0.9486 to 0.9980 for QUI adsorption by anthracite indicating multilayer adsorption on heterogenous surface of adsorbent (Xu et al., 2019). For the QUI adsorption experiment study, it was found that n > 1 which from suggests that the adsorption mechanism of QUI is a reversible process, implying physisorption (Desta, 2013).

The heat of sorption constant , b_T is relatively low at only 3.109 kJ/mol which signifies occurrence of physical and chemical adsorption of QUI on modified AC. The maximum binding energy, A_T at 1.540 l/mg is quite low compared to Wang et al. (2020) research study. They reported A_T value of 5.111 l/mg during adsorption experiment of QUI from wastewater using coke powder. The Temkin adsorption isotherm model does not provide a good fit for the QUI adsorption isotherm model because liquid-phase adsorption isotherms are more complicated, however, it is suitable for gas-phase adsorption system since, particles are free-moving and does not have similar orientation (Amin et al., 2015).

Table 7: Adsorption experiment data for IND concentration

C_o (mg/l)	C_e (mg/l)	V (l)	W (g)	Q_e (mg/g)	Removal Percentage (%)
20.00	2.386	0.1000	1.000	1.761	88.07
40.00	13.58	0.1000	1.000	2.642	66.05
60.00	25.51	0.1000	1.000	3.449	57.49
80.00	43.84	0.1000	1.000	3.616	45.20
100.00	63.91	0.1000	1.000	3.609	36.09

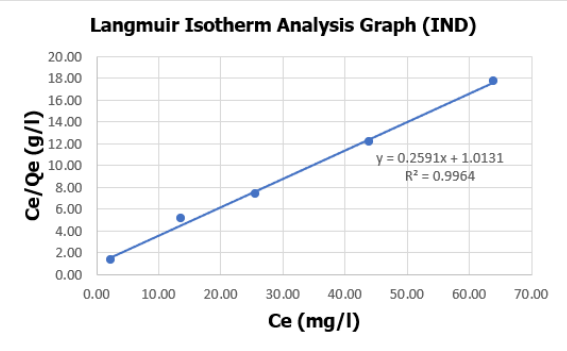

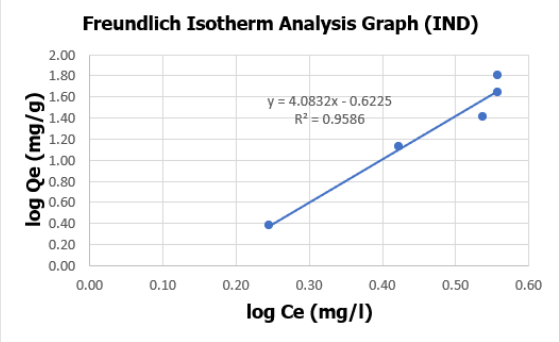

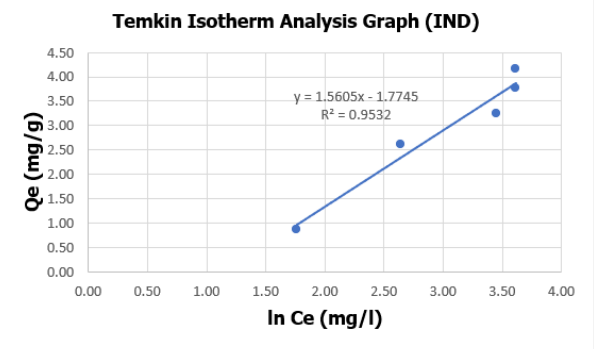

Figure 4: Isotherm analysis for IND adsorption onto 75% H_2SO_4 with $ZnCl_2$ modified AC

All the three isotherm graphs indicated increasing adsorption capacity at equilibrium when equilibrium concentration of IND increased from 20.00mg/l to 100.00 mg/l. This implies that 75% H_2SO_4 and $ZnCl_2$ modified AC is able to successfully adsorb IND compounds from n-hexane. It is also observed that the removal percentage of IND from n-hexane using declines from 88.07% to 36.09% as the equilibrium concentration increased from 20.00 mg/l to 100.00 mg/l. This suggests that adsorption of IND is favourable at low initial concentration of IND. This is due to the fact that the ratio of IND molecules to accessible binding sites on the modified AC is low, hence, indicating a higher probability of interaction between free active sites and IND molecule (Gebreslassie, 2020). On the contrarily, as number of IND molecules increases, the active site on modified AC becomes saturated and is unable to cater to anymore IND molecules, resulting in a drop percentage removal of IND. Another possible reason is the hydrophobic nature of n-hexane, which is heavily absorbed by the modified AC, thus disrupting the efficiency of IND removal (Olajire et al., 2017).

Table 8: Langmuir. Freundlich and Temkin isotherm constants for adsorption of IND from n-hexane

Langmuir's Constants	
K_L (l/mg)	0.2557
Q_{max} (mg/g)	3.860
R_L	0.0391-0.1955
R^2	0.9964
Freundlich's Constants	
K_F (l/mg)	0.2385
n	0.2449
R^2	0.9586
Temkin's Constants	
A_T (l/mg)	0.3207
b_T (kJ/mol)	1.588
R^2	0.9532

The best sequence of the IND adsorption isotherm model for this study slightly differs from DBT and QUI which is Langmuir > Freundlich > Temkin. Similarly, like the DBT and QUI adsorbate, the IND adsorption data is best fitted the Langmuir adsorption isotherm model, because the correlation coefficient, R^2 value at 0.9964 is the closest to 1. According to Langmuir's model, the surface of 75% H_2SO_4 and $ZnCl_2$ modified AC has a specific number of binding sites, where it forms a monolayer of

IND, resulting in inability of future adsorption process to take place. IND adsorption compromises entirely of a monolayer at surface of 30% H_2SO_4 and $ZnCl_2$ modified AC where only one QUI molecule can occupy a single active site.

The Langmuir isotherm constant, K_L which refers to energy and affinity of active site to IND compound were identified to be 0.2557 l/mg which is relatively high. Another research study by Yang et al. (2015), reported a K_L value of 0.0015 for IND adsorption by molecular imprinted polymers. However, this huge difference of values could be the differences in adsorbent material and the surface charge on adsorbent. The separation factor, R_L shows that the adsorption of IND compound onto modified AC is favourable and optimum since it is ranges between 0 to 1. Other studies have also showed that IND adsorption on various adsorbents such as molecular imprinted polymer and acid impregnated metal organic framework had a better fit to Langmuir adsorption isotherm model (Ahmed, Khan, et al., 2013; Yang et al., 2015).

Meanwhile, Anisuzzaman et al. (2018) and Anisuzzaman & Kamarulzaman (2021) found that the adsorption of IND on HCl and H_2SO_4 modified AC fitted Freundlich adsorption isotherm model better with R^2 value closer to 1 at low IND initial concentration range. The value of $n < 1$ from Freundlich isotherm provides information that the adsorption mechanism is a irreversible process, implying chemisorption (Desta, 2013). The energy constant relating to enthalpy of sorption, b_T is relatively low at only 1.588 kJ/mol which implies physisorption and chemisorption process of IND on modified AC. The heat of sorption constant , b_T is relatively low at only 3.109 kJ/mol which signifies occurrence of physical and chemical adsorption of IND on modified AC. The maximum bonding energy, A_T at 1.540 l/mg is higher than of QUI in this research study. The Temkin model is unsuitable to describe the adsorption mechanism of IND on modified AC because it involves liquid-phase adsorption process which is more complex as compared to gas-phase system (Amin et al., 2015).

3.5. Adsorption Kinetic Model Analysis. Adsorption studies using two kinetic models which are pseudo-first order model and pseudo-second order model is conducted to gather significant information on the chemical pathways, adsorption rate and as well as its mechanism of adsorbates onto modified AC. These observations were required to determine the effectiveness of modified AC and to ascertain the best operating parameters for maximum percentage removal of adsorbates.

Table 9: Adsorption kinetic data for DBT concentration

Stirring time (hr)	**C_o (mg/l)**	**C_t (mg/l)**	**Q_t (mg/g)**	**Removal Percentage (%)**

0	100.00	0	0	0
1	100.00	33.54	6.646	66.46
2	100.00	31.92	6.809	68.09
3	100.00	30.38	6.962	69.62
4	100.00	28.32	7.168	71.68
5	100.00	27.81	7.219	72.19

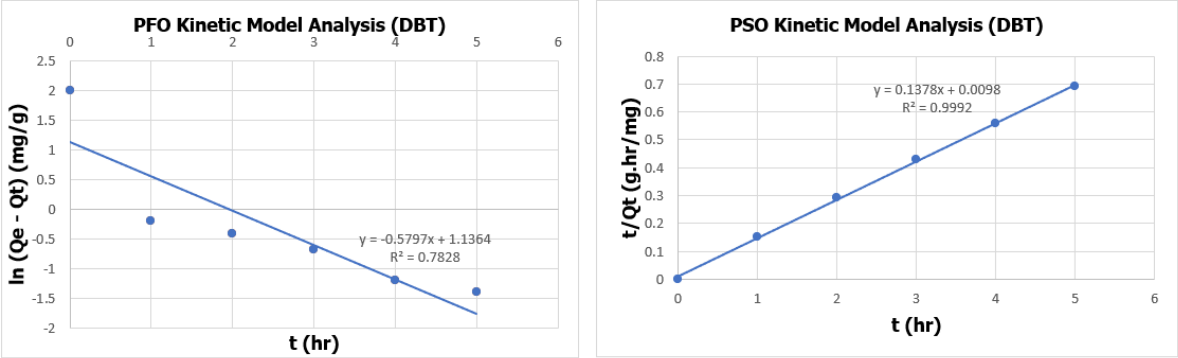

Figure 5: Kinetic model analysis for DBT adsorption onto 75% H_2SO_4 with $ZnCl_2$ modified AC

The DBT data for this adsorption experiment using 75% H_2SO_4 and $ZnCl_2$ modified AC as shown in Table 9 demonstrates that the rate of DBT adsorption was very rapid from 0 to 1 hr, which is attributed to the existence of a significant number of vacant binding site which are accessible to the DBT molecule. However, after 1 hour, the removal percentage of DBT increases slightly after each interval hour. This could be due to the reduction of active sites available for binding with DBT molecule. The results from this experimental study suggest that most of DBT compound is removed within the first hour. Similar results were obtained by Fayazi et al. (2015) during DBT adsorption experiment using magnetic activated carbon which reported high DBT uptake rate within the first interval and then the adsorption rate reached dynamic equilibrium.

Table 10: Pseudo first and second order constants for adsorption of DBT from n-hexane

Pseudo First Order Constants	
K_1 (hr^{-1})	0.5797
$Q_{e(exp)}$ (mg/g)	7.468
$Q_{e(calc)}$ (mg/g)	3.116
R^2	0.7828
Pseudo Second Order Constants	
K_2 (g/mg.hr)	1.938

$Q_{e(exp)}$ (mg/g)	7.468
$Q_{e(calc)}$ (mg/g)	7.257
R^2	0.9992

According to the data in Table 10, the adsorption of DBT from n-hexane using 75% H_2SO_4 and $ZnCl_2$ modified AC fit perfectly into the PSO kinetic model, since it has a higher corelation coefficient, R^2 at 0.9992 which is relatively close to 1 and is linear. This reveals that the chemical interaction between functional groups present on modified AC surface and DBT molecule are a rate determining step (Nazal et al., 2019; Olajire et al., 2017). Moreover, the calculated adsorption capacity, ($Q_{e(calc)}$) value is quite close to the experimental adsorption capacity ($Q_{e(exp)}$) for PFO kinetic model as compared to PSO model. Adding to that, the difference between experimented and calculated adsorption capacity from PSO kinetic model has a percentage error of 58.28%.

The kinetic rate ,K_2, from PSO kinetic model is also higher that than of K_1 in PFO model which means that the adsorption rate of DBT onto modified AC is comparatively faster. It is also discovered that PFO kinetic model has a low R_2 of 0.7828, hence indicating that the adsorption mechanism is not appropriate to be described using PFO kinetic model. The poor R^2 value for PFO kinetic model obtained from the adsorption of DBT onto modified AC had also been reported previously by several research studies (Fayazi et al., 2015; Kumar Thaligari et al., 2018). They concluded that DBT adsorption provided a better fitting to PSO kinetic model relative to the PFO kinetic model. Conversely, activated carbon modified with HNO_3 obeyed PFO kinetic model with DBT adsorption from n-heptane (Anisuzzaman & Maramin, 2021).

Table 11: Adsorption kinetic data for QUI concentration

Stirring time (hr)	**C_o (mg/l)**	**C_t (mg/l)**	**Q_t (mg/g)**	**Removal Percentage (%)**
0	100.00	0	0	0
1	100.00	59.69	4.031	40.31
2	100.00	58.08	4.192	41.92
3	100.00	56.38	4.362	43.62
4	100.00	55.48	4.452	44.52
5	100.00	54.65	4.535	45.35

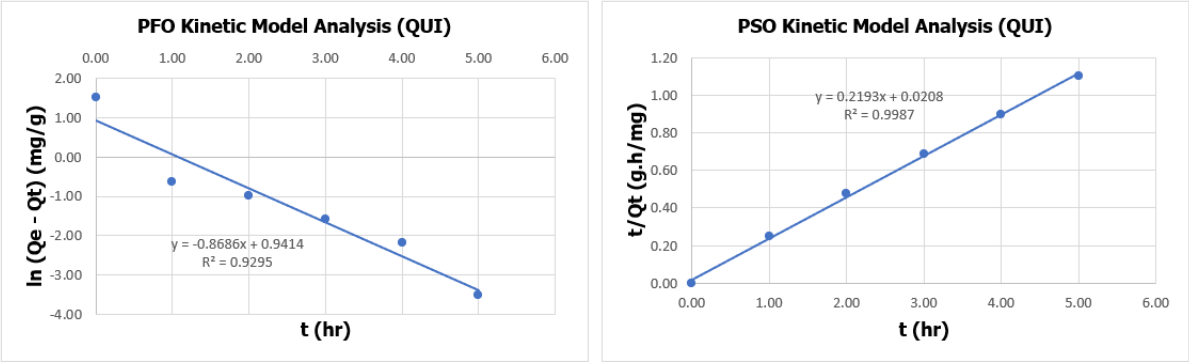

Figure 6: Kinetic model analysis for QUI adsorption onto 30% H_2SO_4 with $ZnCl_2$ modified AC

As shown in Table 11, as the stirring time increases, the concentration of QUI remained in n-hexane reduced almost half from the initial QUI concentration. Not only that, the removal percentage of QUI from n-hexane using 30% H_2SO_4 and $ZnCl_2$ modified AC increased over time. The rate of adsorption was relatively high for the first hour and then increased slightly after each interval to reach 45.35%. The slight increase could be due to fewer binding sites available and the repulsive forces between QUI molecule in solution as well as on modified AC surface. Similar observation on high QUI removal percentage from adsorbent within the first interval were also observed by another researcher (Xu et al., 2019).

Table 12: Pseudo first and second order constants for adsorption of QUI from n-hexane

Pseudo First Order Constants	
K_1 (hr^{-1})	0.8686
$Q_{e(exp)}$ (mg/g)	4.565
$Q_{e(calc)}$ (mg/g)	2.564
R^2	0.9295
Pseudo Second Order Constants	
K_2 (g/mg.hr)	2.312
$Q_{e(exp)}$ (mg/g)	4.565
$Q_{e(calc)}$ (mg/g)	4.560
R^2	0.9987

As listed in Table 12, the R^2 values obtained from PFO and PSO kinetic model are well above 0.90. However, the PSO kinetic model is best to describe the adsorption mechanism of QUI from n-hexane as it has a R^2 value closer to unity. The results indicate that the adsorption process of QUI onto modified AC belongs to chemisorption process (Xu et al., 2019). In addition to that, the difference between the calculated adsorption capacity, ($Q_{e(calc)}$) is very low to the experimental

adsorption capacity ($Q_{e(exp)}$) for PSO kinetic model with only 0.11% error. On the other hand, the ($Q_{e(calc)}$) is much lower than the ($Q_{e(exp)}$) for PFO kinetic model, hence indicating that this kinetic model is unsuitable. The kinetic rate ,K_2, from PSO kinetic model is also higher that than of K_1 in PFO model which means that the adsorption rate of QUI onto modified AC is relatively higher.

The results obtained during this adsorption experiment is similar to the results reported by numerous authors. Xu et al. (2019) described the removal of QUI from wastewater using anthracite and concluded that the kinetic data best fitted the PSO expression. Kumar Thaligari et al. (2018) also concluded that the PSO kinetic model best described the adsorption of QUI from iso-octane onto nickel impregnated granular AC. Adding to that, a study conducted by Wang et al. (2020) on adsorption of aqueous QUI solution by ion impregnated coke powder deduced that the kinetic data provided the best fit to PSO kinetic model. Alves (2019) studied the adsorption of QUI from ethanol onto activated biochar which followed PSO kinetic model as well. On the contrary, activated carbon modified with HCL obeyed PFO kinetic model at low initial QUI concentration around 2 to 10 mg/l (Anisuzzaman & Kamarulzaman, 2021).

Table 13: Adsorption kinetic data for IND concentration

Stirring time (hr)	C_o (mg/l)	C_t (mg/l)	Q_t (mg/g)	Removal Percentage (%)
0	100.00	100.00	0	0
1	100.00	63.91	3.609	36.09
2	100.00	63.82	3.618	36.18
3	100.00	63.56	6.644	36.44
4	100.00	63.16	3.684	36.84
5	100.00	62.82	3.718	37.18

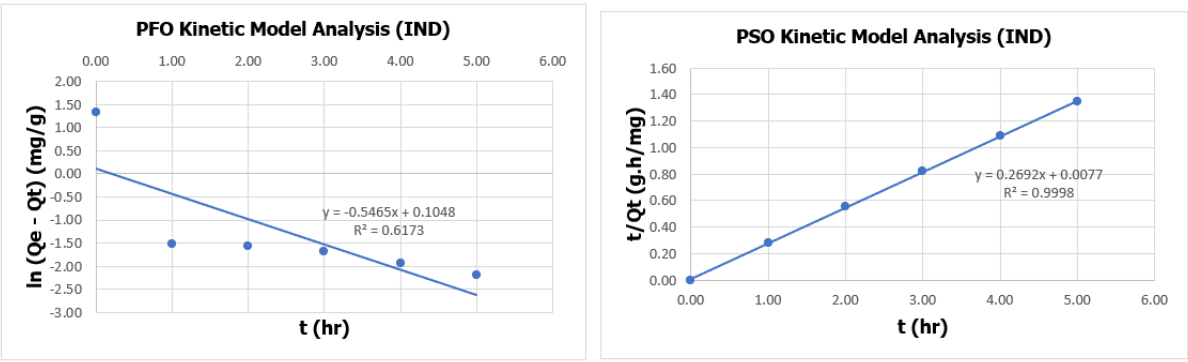

Figure 7: Kinetic model analysis for IND adsorption onto 75% H_2SO_4 with $ZnCl_2$ modified AC

From Table 13, it can be concluded that the concentration of IND left in n-hexane decreases with as stirring time increases. This means that more IND molecule is adsorbed onto 75% H_2SO_4 and $ZnCl_2$ modified AC with respect to stirring time. Besides that, it can be observed from the table that as time increases, the removal percentage of IND from n-hexane using modified AC increases as well. However, the removal percentage of IND is lower than of QUI because IND has a higher nitrogen content, hence more nitrogen molecules need to compete for limited number of active sites on the modified AC (Anisuzzaman et al., 2018). In this experimental study, the rate of adsorption of IND onto modified AC observed high response for the first hour and then slight increment subsequently. This signifies that within the first hour, there are numerous accessible active sites for the binding of IND molecule, but after that, the remaining free IND molecule had to lesser binding sites available due to the modified AC surface being saturated with bonded IND molecule. The same observation was reported by another research study by Anisuzzaman et al. (2018).

Table 14: Pseudo first and second order constants for adsorption of IND from n-hexane

Pseudo First Order Constants	
K_1 (hr^{-1})	0.5465
$Q_{e(exp)}$ (mg/g)	3.828
$Q_{e(calc)}$ (mg/g)	1.111
R^2	0.6173
Pseudo Second Order Constants	
K_2 (g/mg.hr)	9.412
$Q_{e(exp)}$ (mg/g)	3.828
$Q_{e(calc)}$ (mg/g)	3.718
R^2	0.9998

From Table 14, it can be concluded that the adsorption of IND from n-hexane using 75% H_2SO_4 and $ZnCl_2$ modified AC has a better fitting to the PSO kinetic model since the correlation coefficient, R^2 is closer to 1 (>0.99) as compared to PFO kinetic model. Therefore, this implies that the chemisorption takes place as the adsorption mechanism of IND from n-hexane (Sahoo & Prelot, 2020). The R^2 values obtained from PFO kinetic model were below 0.99, hence this verifies that PFO is inappropriate to describe the adsorption mechanism. Moreover, the calculated adsorption capacity, ($Q_{e(calc)}$) for PFO kinetic model has a huge difference with the experimental adsorption capacity ($Q_{e(exp)}$) with up to 70. 98% differences. Meanwhile, the PFO kinetic model presented smaller discrepancies between $Q_{e(calc)}$ and $Q_{e(exp)}$. The kinetic rate ,K_2, from PSO kinetic model is also much

higher that than of K_1 in PFO model which means that the adsorption rate of IND onto modified AC is relatively higher.

The results obtained from this experimental study were similar to the findings of other researchers. Anisuzzaman et al. (2018) deduced that the adsorption of IND from model fuel using various H_2SO_4 concentration to modify AC obeyed PSO kinetic model with R^2 value ranging from 0.9701 to 0.9962. In addition to that, the adsorption performance of IND using molecular imprinted polymer also suggested a better fitting to the PSO kinetic model instead of the PFO kinetic model (Yang et al., 2015). Similarly, the PSO kinetic model was a better fit do the IND adsorption data reported by Devidas Hiwarkar et al. (2014), who studied the adsorption IND using bagasse fly ash and granular AC. On the other hand, a study by Anisuzzaman & Kamarulzaman (2021) concluded that activated carbon modified with HCL obeyed PFO kinetic model at low initial IND concentration around 2 to 10 mg/l.

4. Conclusion

In summary, this research study revealed that double impregnation using H_2SO_4 followed by $ZnCl_2$ significantly increased the percentage removal of DBT, QUI and IND as compared to raw AC. To be more specific, DBT and IND showed high percentage removal up to 86.23% and 82.77% respectively using 75% H_2SO_4 with $ZnCl_2$ modified AC. Meanwhile, QUI favoured 30% H_2SO_4 with $ZnCl_2$ modified AC with percentage removal of 33.17% which is still higher than unmodified AC. Characterization study including percentage yield, pH, bulk density, moisture content, ash content, and iodine number were also conducted.

From these characterization tests, it was observed that high percentage yield was obtained which are 72.08% and 71.13% for 30% and 75% H_2SO_4 and $ZnCl_2$ modified AC respectively.=. The pH tested were also within the acidic range below 6 even after washing steps. Bulk densities were also favourable while the moisture and ash content were within acceptable limits. Iodine number test showed that the modified AC achieved high porosity and good adsorption performance. In addition, the FTIR spectra of modified AC revealed that H_2SO_4 were successfully introduced since there are presence of S-H thiol and free O-H group only after modification step.

The empirical adsorption relationship between modified AC, adsorbate molecules and adsorption mechanism at equilibrium were described using Langmuir, Freundlich and Temkin isotherm models. It is concluded that DBT, QUI and IND followed Langmuir isotherm model better with correlation coefficient, R^2 of 0.9905, 0.9791 and 0.9964 respectively. Moreover, the adsorption kinetic data of DBT, QUI and IND provided a better fitting to pseudo-second order kinetic model with R^2 of 0.9992, 0.9987 and 0.9998 respectively.

References

[1] Ahmed, I., Hasan, Z., Khan, N. A., & Jhung, S. H. (2013). Adsorptive denitrogenation of model fuels with porous metal-organic frameworks (MOFs): Effect of acidity and basicity of MOFs. *Applied Catalysis B: Environmental*, *129*, 123–129. https://doi.org/10.1016/j.apcatb.2012.09.020

[2] Ahmed, I., Khan, N. A., Hasan, Z., & Jhung, S. H. (2013). Adsorptive denitrogenation of model fuels with porous metal-organic framework (MOF) MIL-101 impregnated with phosphotungstic acid: Effect of acid site inclusion. *Journal of Hazardous Materials*, *250–251*, 37–44. https://doi.org/10.1016/j.jhazmat.2013.01.024

[3] Almarri, M., Ma, X., & Song, C. (2009). Selective adsorption for removal of nitrogen compounds from liquid hydrocarbon streams over carbon- and alumina-based adsorbents. *Industrial and Engineering Chemistry Research*, *48*(2), 951–960. https://doi.org/10.1021/ie801010w

[4] Alves, G. G. (2019). *Removal of quinoline from oily wastewater using biochars prepared from compost*.

[5] Amin, M. T., Alazba, A. A., & Shafiq, M. (2015). Adsorptive removal of reactive black 5 from wastewater using bentonite clay: Isotherms, kinetics and thermodynamics. *Sustainability (Switzerland)*, *7*(11), 15302–15318. https://doi.org/10.3390/su71115302

[6] Angin, D. (2014). Production and characterization of activated carbon from sour cherry stones by zinc chloride. *Fuel*, *115*, 804–811. https://doi.org/10.1016/j.fuel.2013.04.060

[7] Anisuzzaman, S. M., Joseph, C. G., Taufiq-Yap, Y. H., Krishnaiah, D., & Tay, V. v. (2015a). Modification of commercial activated carbon for the removal of 2,4-dichlorophenol from simulated wastewater. *Journal of King Saud University - Science*, *27*(4), 318–330. https://doi.org/10.1016/j.jksus.2015.01.002

[8] Anisuzzaman, S. M., Joseph, C. G., Taufiq-Yap, Y. H., Krishnaiah, D., & Tay, V. v. (2015b). Modification of commercial activated carbon for the removal of 2,4-dichlorophenol from simulated wastewater. *Journal of King Saud University - Science*, *27*(4), 318–330. https://doi.org/10.1016/j.jksus.2015.01.002

[9] Anisuzzaman, S. M., & Kamarulzaman, S. (2021). Removal of Nitrogen Containing Compounds From Fuel Using Modified Activated Carbon. In *2021. Transactions on Science and Technology* (Vol. 8, Issue 1). http://tost.unise.org/

[10] Anisuzzaman, S. M., Krishnaiah, D., & Alfred, D. (2018). Adsorption potential of a modified activated carbon for the removal of nitrogen containing compounds from model fuel. *AIP Conference Proceedings*, *1930*. https://doi.org/10.1063/1.5022907

[11] Anisuzzaman, S. M., & Maramin, N. A. (2021). Adsorptive Desulfurization of Model Fuel by Modified Activated Carbon. In *Malaysian Journal of Chemistry* (Vol. 23, Issue 3).

[12] Awe, A. A., Opeolu, B. O., Fatoki, O. S., Ayanda, O. S., Jackson, V. A., & Snyman, R. (2020). Preparation and characterisation of activated carbon from Vitis vinifera leaf litter and its adsorption performance for aqueous phenanthrene. *Applied Biological Chemistry*, *63*(1). https://doi.org/10.1186/s13765-020-00494-1

[13] Ayawei, N., Ebelegi, A. N., & Wankasi, D. (2017). Modelling and Interpretation of Adsorption Isotherms. In *Journal of Chemistry* (Vol. 2017). Hindawi Limited. https://doi.org/10.1155/2017/3039817

[14] Bansal, R. C., & Goyal, Meenakshi. (2005). *Activated carbon adsorption*. Taylor & Francis.

[15] Bouchemal, N., Belhachemi, M., Merzougui, Z., & Addoun, F. (2009). The effect of temperature and impregnation ratio on the active carbon porosity. *Desalination and Water Treatment*, *10*(1–3), 115–120. https://doi.org/10.5004/dwt.2009.828

[16] Chandra Srivastava, V. (2012). An evaluation of desulfurization technologies for sulfur removal from liquid fuels. In *RSC Advances* (Vol. 2, Issue 3, pp. 759–783). https://doi.org/10.1039/c1ra00309g

[17] Desta, M. B. (2013). Batch sorption experiments: Langmuir and freundlich isotherm studies for the adsorption of textile metal ions onto teff straw (eragrostis tef) agricultural waste. *Journal of Thermodynamics*, *1*(1). https://doi.org/10.1155/2013/375830

[18] Devidas Hiwarkar, A., Srivastava, C., & Deo, I. (2014). *Comparative Studies on Adsorptive Removal of Indole by Granular Activated Carbon and Bagasse Fly Ash*. *34*, 492–503. https://doi.org/10.1002/ep.12025

[19] Efeovbokhan, V. E., Alagbe, E. E., Odika, B., Babalola, R., Oladimeji, T. E., Abatan, O. G., & Yusuf, E. O. (2019). Preparation and characterization of activated carbon from plantain peel and coconut shell using biological activators. *Journal of Physics: Conference Series*, *1378*(3). https://doi.org/10.1088/1742-6596/1378/3/032035

[20] Fayazi, M., Taher, M. A., Afzali, D., & Mostafavi, A. (2015). Removal of dibenzothiophene using activated carbon/γ-Fe2O3 nano-composite: Kinetic and thermodynamic investigation of the removal process. *Analytical and Bioanalytical Chemistry Research*, *2*(2), 73–84. https://doi.org/10.22036/abcr.2015.10158

[21] Gebreslassie, Y. T. (2020). *Equilibrium, Kinetics, and Thermodynamic Studies of Malachite Green Adsorption onto Fig (Ficus cartia) Leaves*. https://doi.org/10.1155/2020/7384675

[22] Gunorubon Dagde, J., & Kekpugile, K. (2018). *Effect of Activation Method and Agent on the Characterization of Prewinkle Shell Activated Carbon* (Vol. 56). Online. www.iiste.org

[23] Ha, J. W., Japhe, T., Demeke, T., Moreno, B., & Navarro, A. E. (2019). On the Removal and Desorption of Sulfur Compounds from Model Fuels with Modified Clays. *Clean Technologies*, *1*(1), 58–69. https://doi.org/10.3390/cleantechnol1010005

[24] Iwanow, M., Gärtner, T., Sieber, V., & König, B. (2020). Activated carbon as catalyst support: Precursors, preparation, modification and characterization. In *Beilstein Journal of Organic Chemistry* (Vol. 16, pp. 1188–1202). Beilstein-Institut Zur Forderung der Chemischen Wissenschaften. https://doi.org/10.3762/bjoc.16.104

[25] Jawad, A. H., Rashid, R. A., Ishak, M. A. M., & Wilson, L. D. (2016). Adsorption of methylene blue onto activated carbon developed from biomass waste by H2SO4 activation: kinetic, equilibrium and thermodynamic studies. *Desalination and Water Treatment*, *57*(52), 25194–25206. https://doi.org/10.1080/19443994.2016.1144534

[26] Jeyakumar, R. P. S., & Chandrasekaran, V. (2014). Preparation and characterization of activated carbons derived from marine green algae ulva fasciata sp. *Asian Journal of Chemistry*, *26*(9), 2545–2549. https://doi.org/10.14233/ajchem.2014.15723

[27] Kumar Thaligari, S., Gupta, S., Srivastava, V. C., & Prasad, B. (2018). Adsorptive desulfurization and denitrogenation by nickel impregnated activated carbon. In *Indian Journal of Chemical Technology* (Vol. 25).

[28] Lee, S. H. D., Kumar, R., & Krumpelt, M. (2002). Sulfur removal from diesel fuel-contaminated methanol. In *Separation and Purification Technology* (Vol. 26). www.elsevier.com/locate/seppur

[29] Lesaoana, M., Mlaba, R. P. V., Mtunzi, F. M., Klink, M. J., Edijike, P., & Pakade, V. E. (2019). Influence of inorganic acid modification on Cr(VI) adsorption performance and the physicochemical properties of activated carbon. In *South African Journal of Chemical Engineering* (Vol. 28, pp. 8–18). Elsevier B.V. https://doi.org/10.1016/j.sajce.2019.01.001

[30] Lopes, A. R., Scheer, A. de P., Silva, G. V., & Yamamoto, C. I. (2016). Pd-Impregnated activated carbon and treatment acid to remove sulfur and nitrogen from

diesel. *Revista Materia*, *21*(2), 407–415. https://doi.org/10.1590/S1517-707620160002.0038

[31] Martínez-Mendoza, K. L., Barraza-Burgos, J. M., Marriaga-Cabrales, N., Machuca-Martinez, F., Barajas, M., & Romero, M. (2020). Production and characterization of activated carbon from coal for gold adsorption in cyanide solutions. *Ingenieria e Investigacion*, *40*(1), 34–44. https://doi.org/10.15446/ing.investig.v40n1.80126

[32] Mkungunugwa, T., Manhokwe, S., Chawafambira, A., & Shumba, M. (2021). Synthesis and Characterisation of Activated Carbon Obtained from Marula (Sclerocarya birrea) Nutshell. *Journal of Chemistry*, *2021*. https://doi.org/10.1155/2021/5552224

[33] Mopoung, S., Moonsri, P., Palas, W., & Khumpai, S. (2015). Characterization and Properties of Activated Carbon Prepared from Tamarind Seeds by KOH Activation for Fe(III) Adsorption from Aqueous Solution. *Scientific World Journal*, *2015*. https://doi.org/10.1155/2015/415961

[34] Nazal, M. K., Khaled, M., Atieh, M. A., Aljundi, I. H., Oweimreen, G. A., & Abulkibash, A. M. (2019). The nature and kinetics of the adsorption of dibenzothiophene in model diesel fuel on carbonaceous materials loaded with aluminum oxide particles. *Arabian Journal of Chemistry*, *12*(8), 3678–3691. https://doi.org/10.1016/j.arabjc.2015.12.003

[35] Olajire, A. A., Abidemi, J. J., Lateef, A., & Benson, N. U. (2017a). Adsorptive desulphurization of model oil by Ag nanoparticles-modified activated carbon prepared from brewer's spent grains. *Journal of Environmental Chemical Engineering*, *5*(1), 147–159. https://doi.org/10.1016/j.jece.2016.11.033

[36] Olajire, A. A., Abidemi, J. J., Lateef, A., & Benson, N. U. (2017b). Adsorptive desulphurization of model oil by Ag nanoparticles-modified activated carbon prepared from brewer's spent grains. *Journal of Environmental Chemical Engineering*, *5*(1), 147–159. https://doi.org/10.1016/j.jece.2016.11.033

[37] Owabor, C., & Iyaomolere, A. (2013). Evaluation of the Influence of Salt Treatment on the Structure of Pyrolyzed Periwinkle Shell. *Journal of Applied Sciences and Environmental Management*, *17*(2). https://doi.org/10.4314/jasem.v17i2.15

[38] Pratumpong, P., & Toommee, S. (2016). Utilization of zinc chloride for surface modification of activated carbon derived from Jatropha curcas L. for absorbent material. *Data in Brief*, *9*, 970–975. https://doi.org/10.1016/j.dib.2016.11.019

[39] Qu, D., Feng, X., Li, N., Ma, X., Shang, C., & Chen, X. D. (2016). Adsorption of heterocyclic sulfur and nitrogen compounds in liquid hydrocarbons on activated carbons modified by oxidation: Capacity, selectivity and mechanism. *RSC Advances*, *6*(48), 41982–41990. https://doi.org/10.1039/c6ra06108g

[40] Sahoo, T. R., & Prelot, B. (2020). Adsorption processes for the removal of contaminants from wastewater: the perspective role of nanomaterials and nanotechnology. *Nanomaterials for the Detection and Removal of Wastewater Pollutants*, 161–222. https://doi.org/10.1016/B978-0-12-818489-9.00007-4

[41] Sarker, M., An, H. J., & Jhung, S. H. (2018). Adsorptive Removal of Indole and Quinoline from Model Fuel over Various UiO-66s: Quantitative Contributions of H-Bonding and Acid-Base Interactions to Adsorption. *Journal of Physical Chemistry C*, *122*(8), 4532–4539. https://doi.org/10.1021/acs.jpcc.8b00761

[42] Seredych, M., Lison, J., Jans, U., & Bandosz, T. J. (2009). Textural and chemical factors affecting adsorption capacity of activated carbon in highly efficient desulfurization of diesel fuel. *Carbon*, *47*(10), 2491–2500. https://doi.org/10.1016/j.carbon.2009.05.001

[43] Shafiq, M., Shaid, H. M., Abbas, M., Zaini, A., & Shawal Nasri, N. (2017). Isotherm studies of methylene blue adsorption onto waste tyre pyrolysis powder-based activated carbons Article history. In */ Malaysian Journal of Fundamental and Applied Sciences* (Vol. 13, Issue 4).

[44] Suhdi, & Wang, S. C. (2021). Fine activated carbon from rubber fruit shell prepared by using zncl2 and koh activation. *Applied Sciences (Switzerland)*, *11*(9). https://doi.org/10.3390/app11093994

[45] Tsai, C. Y., Chiu, C. H., Chuang, M. W., & Hsi, H. C. (2017). Influences of copper(II) chloride impregnation on activated carbon for low-concentration elemental mercury adsorption from simulated coal combustion flue gas. *Aerosol and Air Quality Research*, *17*(6), 1537–1548. https://doi.org/10.4209/aaqr.2016.10.0435

[46] von Mühlen, C., de Oliveira, E. C., Zini, C. A., Caramão, E. B., & Marriott, P. J. (2010). Characterization of nitrogen-containing compounds in heavy gas oil petroleum fractions using comprehensive two-dimensional gas chromatography coupled to time-of-flight mass spectrometry. *Energy and Fuels*, *24*(6), 3572–3580. https://doi.org/10.1021/ef1002364

[47] Wang, L., Gao, Q., Li, Z., & Wang, Y. (2020). Improved removal of quinoline from wastewater using coke powder with inorganic ions. *Processes*, *8*(2). https://doi.org/10.3390/PR8020156

[48] Wang, Y., & Yang, R. T. (2007). Desulfurization of liquid fuels by adsorption on carbon-based sorbents and ultrasound-assisted sorbent regeneration. *Langmuir*, *23*(7), 3825–3831. https://doi.org/10.1021/la063364z

[49] Xu, H., Sun, X., Yu, Y., Liu, G., Ma, L., & Huang, G. (2019). Removal of quinoline using various particle sizes anthracite: Adsorption kinetics and adsorption isotherms. *Physicochemical Problems of Mineral Processing*, *55*(1), 196–207. https://doi.org/10.5277/ppmp18121

[50] Yahya, M. A., Al-Qodah, Z., & Ngah, C. W. Z. (2015). Agricultural bio-waste materials as potential sustainable precursors used for activated carbon production: A review. In *Renewable and Sustainable Energy Reviews* (Vol. 46, pp. 218–235). Elsevier Ltd. https://doi.org/10.1016/j.rser.2015.02.051

[51] Yakub, I., Mohammad, M., & Yaakob, Z. (2013). Effects of zinc chloride impregnation on the characteristics of activated carbon produced from physic nut seed hull. *Advanced Materials Research*, *626*, 751–755. https://doi.org/10.4028/www.scientific.net/AMR.626.751

[52] Yang, W., Cao, Y., Ni, X., Hunag, W., & Xu, W. (2015). *Synthesis of a Denitrification Adsorbent with Large Surface Area and Specific Pore Structure for the Removal of Indole from Fuel Oil*.

[53] Yusufu M. I. (2012). Production and characterization of activated carbon from selected local raw materials. *African Journal of Pure and Applied Chemistry*, *6*(9). https://doi.org/10.5897/ajpac12.022

[54] Zhou, L., Li, M., Sun, Y., & Zhou, Y. (2001). Effect of moisture in microporous activated carbon on the adsorption of methane. *Carbon*, *39*, 773–776.

[55] Zulkania, A., Hanum, G. F., & Sri Rezki, A. (2018). The potential of activated carbon derived from bio-char waste of bio-oil pyrolysis as adsorbent. *MATEC Web of Conferences*, *154*. https://doi.org/10.1051/matecconf/201815401029